Time-dependent space-charge-limited conduction as a possible origin of the polarization offsets observed in compositionally graded ferroelectric films

H. K. Chan,[a] C. H. Lam, and F. G. Shin
Department of Applied Physics, The Hong Kong Polytechnic University, Hong Kong, China

(Received 3 October 2003; accepted 19 December 2003)

We investigated the effects of free space charges on hysteresis-loop measurement of compositionally graded ferroelectrics and found that they are quite likely to be responsible for the ''polarization offsets'' observed in experiments. Taking into account conduction by those free space charges, or time-dependent space-charge-limited conduction, our computer simulation of compositionally graded lead zirconate titanate, which is placed in the Sawyer–Tower circuit and driven by an alternating applied voltage, produced shifting of measured hysteresis loops where the shift magnitudes are comparable with published experimental data. It also produced the key features as observed in experiments: The ''offsets:'' (a) have a monotonous increase with electric-field amplitude, (b) change in direction when the composition gradient is inverted, and (c) develop like the typical charging-up of a capacitor. All these results suggest that time-dependent space-charge-limited conduction is a possible origin of the polarization offsets observed in compositionally graded ferroelectrics. © *2004 American Institute of Physics.*
[DOI: 10.1063/1.1647258]

I. INTRODUCTION

The history of extensive research on compositionally graded ferroelectrics dates back to the early 1990s when Mantese *et al.*[1] discovered the vertical shifting of measured $D-E$ hysteresis loops in potassium tantalum niobate films graded in potassium concentration, placed in a Sawyer–Tower circuit,[2] and driven by an alternating voltage. This is the so-called ''charge-pumping'' effect or ''polarization offset,'' from which a strong dependence on electric field and temperature was reported.[1] Since then, the same effect has been observed on a wide range of compositionally graded ferroelectric films,[3–12] where in many cases the shift displayed a power 3–5 dependence on the electric-field amplitude[3,4,5,7,9,11,12] and changed in a direction[3–5] when the composition gradient was inverted. Brazier *et al.* showed that the offset develops like the typical charging-up of a capacitor, with the time constant approximately equal to the product of its capacitance and input impedance.[13] All these features have made graded ferroelectrics a very attractive class of materials because of its potential device applications, and hence, have urged for a greater understanding of them.

There have been various ideas suggesting possible origins of the shift. As its name suggests, the shift or polarization offset has been interpreted as a static polarization developed across the ferroelectric film under the application of an alternating voltage.[4] However, those ''offsets'' are usually almost an order of magnitude larger than the typical spontaneous polarization of the material, and hence, such a large static component is not likely to occur.[13] This has been followed by an alternative idea that the shift should correspond to a static voltage developed across the ferroelectric film under the application of the alternating voltage; yet the origin of this static voltage remains unclear.[13] Recently it has been proposed with experimental support that the shift should originate from the asymmetrical current–voltage characteristics of the ferroelectric film; the relation of such asymmetry with the composition gradient of the film has yet not been understood.[3,14] There has not been any theoretical model that satisfactorily explains the origin of the shift as well as its dependence on electric field and temperature.

On the other hand, it is worth also considering the fact that similar shifting of hysteresis loops has been observed when the compositionally graded sample was replaced by a homogeneous one across which a thermal (temperature) gradient was imposed.[15] Since the shift vanished with the removal of the thermal gradient, it is likely that such shifting arises from the thermally induced gradient in polarization[15,16] or, more generally, electric displacement which, according to Gauss' law, represents the presence of free space charges in the sample. It follows that, if the shifts from compositional and thermal gradients are of the same origin, the vertical shifting of hysteresis loops in compositionally graded ferroelectrics might originate from conduction by those free space charges.

In this article, we derive an expression for the conduction–current density associated with those free space charges and present our numerical investigation of their effects on hysteresis-loop measurement of compositionally graded ferroelectrics, particularly of whether they are responsible for those polarization offsets observed in experiments.

[a]Electronic mail: hokei@superhome.net

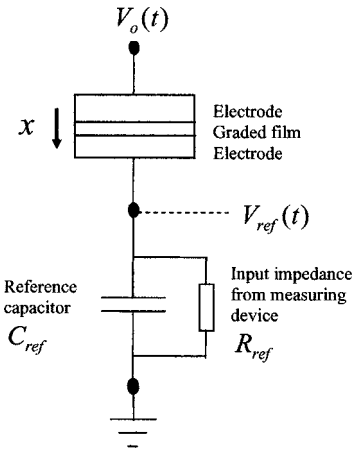

FIG. 1. Schematic diagram of the Sawyer–Tower circuit.

II. TIME-DEPENDENT SPACE-CHARGE-LIMITED CONDUCTION

For a compositionally graded ferroelectric film placed in a Sawyer–Tower circuit (see Fig. 1) and driven by an alternating voltage $V_0(t)$, its conduction–current density $J_c(x,t)$, electric field $E(x,t)$, switchable polarization $P(x,t)$ and electric displacement $D(x,t)$, are functions of position x and time t. For the sake of generality and simplicity, respectively, we relate the conduction–current density to the electric field via a time-dependent conductivity $\sigma(x,t)$ and ignore carrier diffusion

$$J_c(x,t)=\sigma(x,t)E(x,t). \tag{1}$$

For simplicity, we assume the ferroelectric film consists of p-type and n-type free carriers whose mobilities μ_p and $-\mu_n$ (μ_p, $\mu_n>0$) are uniform across the film and whose electric charges are equal to q and $-q$ ($q>0$), respectively. Due to charge neutrality, the intrinsic concentrations of the two carrier types are equal and thus both denoted by $C_{\text{in}}(x)$. The time-dependent conductivity can be expressed as

$$\sigma(x,t)=(-q)(-\mu_n)[C_{\text{in}}(x)+\Delta n(x,t)]+q\mu_p[C_{\text{in}}(x)+\Delta p(x,t)], \tag{2}$$

where $\Delta p(x,t)$ and $\Delta n(x,t)$ are, respectively, the differences between intrinsic and total concentrations for each carrier type. Putting the intrinsic conductivity $\sigma_0(x)=q(\mu_n+\mu_p)C_{\text{in}}(x)$ into Eq. (2) yields

$$\sigma(x,t)=\sigma_0(x)+q[\mu_n\Delta n(x,t)+\mu_p\Delta p(x,t)]. \tag{3}$$

According to Gauss' law, the density of free space-charge is given by

$$\frac{\partial D(x,t)}{\partial x}=q[C_{\text{in}}(x)+\Delta p(x,t)]-q[C_{\text{in}}(x)+\Delta n(x,t)]. \tag{4}$$

In practice, the frequency of applied voltage is not too high (usually about 1 kHz) such that, from the quasistatic point of view, the ferroelectric material is approximately at equilibrium for every time instant. Hence, we may apply the law of mass action to describe its carrier concentrations

$$C_{\text{in}}(x)^2=[C_{\text{in}}(x)+\Delta n(x,t)][C_{\text{in}}(x)+\Delta p(x,t)]. \tag{5}$$

From Eqs. (4) and (5), we write

$$\Delta p(x,t)=\frac{1}{q}\frac{\partial D(x,t)}{\partial x}+\Delta n(x,t), \tag{6}$$

$$C_{\text{in}}(x)[\Delta p(x,t)+\Delta n(x,t)]+\Delta n(x,t)\Delta p(x,t)=0 \tag{7}$$

and get

$$\Delta n(x,t)^2+\Delta n(x,t)B_n(x,t)+C_n(x,t)=0, \tag{8}$$

$$\Delta p(x,t)^2+\Delta p(x,t)B_p(x,t)+C_p(x,t)=0, \tag{9}$$

where $B_n(x,t)=\frac{1}{q}\frac{\partial D(x,t)}{\partial x}+2C_{\text{in}}(x)$, $C_n(x,t)=\frac{C_{\text{in}}(x)}{q}\frac{\partial D(x,t)}{\partial x}$,

$B_p(x,t)=-\frac{1}{q}\frac{\partial D(x,t)}{\partial x}+2C_{\text{in}}(x)$ and $C_p(x,t)=-\frac{C_{\text{in}}(x)}{q}\frac{\partial D(x,t)}{\partial x}$,

so that

$$q[\mu_n\Delta n(x,t)+\mu_p\Delta p(x,t)]=q\mu_n\frac{-B_n(x,t)\pm\sqrt{B_n(x,t)^2-4C_n(x,t)}}{2}+q\mu_p\frac{-B_p(x,t)\pm\sqrt{B_p(x,t)^2-4C_p(x,t)}}{2}. \tag{10}$$

It can be shown that

$$-q[\mu_nB_n(x,t)+\mu_pB_p(x,t)]=(\mu_p-\mu_n)\frac{\partial D(x,t)}{\partial x}-2\sigma_0(x), \tag{11}$$

$$q\sqrt{B_n(x,t)^2-4C_n(x,t)}=q\sqrt{B_p(x,t)^2-4C_p(x,t)}=\sqrt{\left[\frac{\partial D(x,t)}{\partial x}\right]^2+\frac{4\sigma_0(x)^2}{(\mu_n+\mu_p)^2}}. \tag{12}$$

Hence, Eq. (10) can be written as

$$q[\mu_n\Delta n(x,t)+\mu_p\Delta p(x,t)]=\frac{\mu_p-\mu_n}{2}\frac{\partial D(x,t)}{\partial x}-\sigma_0(x)+\frac{\pm\mu_n\pm\mu_p}{2}\sqrt{\left[\frac{\partial D(x,t)}{\partial x}\right]^2+\frac{4\sigma_0(x)^2}{(\mu_n+\mu_p)^2}}. \tag{13}$$

Only the root of all upper positive signs is valid because when $\Delta n(x,t)=\Delta p(x,t)=0$, we have $\partial D(x,t)/\partial x=0$ and $\sigma_0(x)=(\pm\mu_n\pm\mu_p)/(\mu_n+\mu_p)\,\sigma_0(x)$. Hence, from Eq. (3):

$$\sigma(x,t)=\frac{\mu_p-\mu_n}{2}\frac{\partial D(x,t)}{\partial x}+\sqrt{\left[\frac{\mu_n+\mu_p}{2}\frac{\partial D(x,t)}{\partial x}\right]^2+\sigma_0(x)^2}. \tag{14}$$

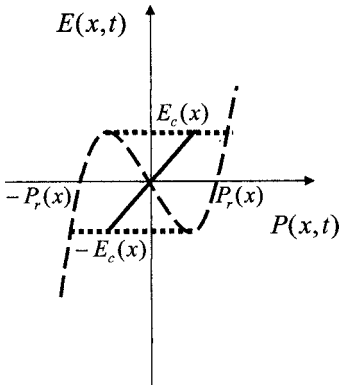

FIG. 2. The $E(x,t)-P(x,t)$ path assigned from the Landau–Devonshire model description. The dashed line represents the Landau–Devonshire electric field $E_L(x,t)$; the dotted lines represent the paths during polarization reversal at $\pm E_c(x)$; and the solid line represents the additional path joining the origin and the major loop.

Note that Eq. (14) can be approximated to a time-independent, single-carrier case with negligible intrinsic conduction by taking either $\mu_p \to 0$ or $\mu_n \to 0$, from which Mott's equation for steady-state space-charge-limited conduction is derived;[17] hence, we call it ''time-dependent space-charge-limited conduction'' to distinguish between the two.

III. METHOD OF NUMERICAL SIMULATION

For a graded ferroelectric film, the electric displacement at position x can be written as

$$D(x,t)=\varepsilon(x)E(x,t)+P(x,t), \tag{15}$$

where $\varepsilon(x)$ is the dielectric permittivity and $P(x,t)$ has a complicated relation with $E(x,t)$. This way of writing the electric displacement has been used previously for homogeneous and multilayer ferroelectric films.[18–20] For simplicity, we borrow the Landau–Devonshire model description[21] with the power 5 and higher-order terms of $P(x,t)$ omitted for assigning $E(x,t)-P(x,t)$ paths inside the graded ferroelectric film. With the film divided into N layers, the Landau–Devonshire electric field that corresponds to the ith layer is

$$E_L(x,t)=\alpha(x)P(x,t)+\beta(x)P(x,t)^3, \tag{16}$$

where $x=i\cdot\Delta x$. The parameters $\alpha(x)$ (<0) and $\beta(x)$ (>0) are calculated from the otherwise obtained remanent polarization $P_r(x)$ and coercive field $E_c(x)$ via Eqs. (17) and (18) (see Appendix A for derivation)

$$\beta(x)=\frac{3\sqrt{3}E_c(x)}{2P_r(x)^3}, \tag{17}$$

$$\alpha(x)=-\beta(x)P_r(x)^2. \tag{18}$$

The actual $E(x,t)-P(x,t)$ path does not completely follow Eq. (16) because it includes polarization reversal at the coercive-field strengths such that a complete hysteresis loop (major loop) is assigned (see Fig. 2). At $t=0$, the material is not polarized and $E(x,t)$ is zero; hence, an additional path is needed for the layer to move from the origin to the major loop when $E(x,t)$ increases or decreases from zero during the first half-cycle (see Fig. 2). As the Landau–Devonshire model description does not provide any well-known information about this additional path, we choose to assign it arbitrarily. Several runs of the computer program show that this additional path does not impose any significant effects on the final results.

In real hysteresis-loop measurement, the voltage $V_{\text{ref}}(t)$ of the reference capacitor is recorded against the average electric field $E_{\text{ave}}(t)$ across the ferroelectric film which is given by $[V_0(t)-V_{\text{ref}}(t)]/L_{\text{ferro}}$, where L_{ferro} is the film thickness. From the circuital point of view, we take into account the continuity of total current

$$J_0(t)=J_c(x,t)+\frac{\partial D(x,t)}{\partial t}=\frac{V_{\text{ref}}(t)}{R_{\text{ref}}A_{\text{ferro}}}+\frac{C_{\text{ref}}}{A_{\text{ferro}}}\frac{dV_{\text{ref}}(t)}{dt} \tag{19}$$

and the vanishing of voltage sum around a closed loop

$$V_0(t)=\int_0^{L_{\text{ferro}}}E(x,t)dx+V_{\text{ref}}(t), \tag{20}$$

where C_{ref} and R_{ref} are, respectively, the capacitance and input impedance of the reference capacitor, A_{ferro} is the electrode area on the ferroelectric film (see Fig. 1), and $J_0(t)$ is the total-current density across the film. Based on Eqs. (15), (19), and (20), we derive an expression (see Appendix B for derivation) for computing $V_{\text{ref}}(t)$ via the forward Euler method

$$V_{\text{ref}}(t+\Delta t)-V_{\text{ref}}(t)=[f_1(t)-V_{\text{ref}}(t)f_2(t)]\Delta t, \tag{21}$$

where

$$f_1(t)=\frac{\dfrac{dV_0(t)}{dt}+\Sigma_{i=1}^{N}\left[\dfrac{J_c(x,t)\dfrac{\partial E(x,t)}{\partial P(x,t)_x}}{1+\varepsilon(x)\dfrac{\partial E(x,t)}{\partial P(x,t)_x}}\Delta x\right]}{1+\dfrac{C_{\text{ref}}}{A_{\text{ferro}}}\Sigma_{i=1}^{N}\left[\dfrac{\dfrac{\partial E(x,t)}{\partial P(x,t)_x}}{1+\varepsilon(x)\dfrac{\partial E(x,t)}{\partial P(x,t)_x}}\Delta x\right]} \quad \text{and}$$

$$f_2(t)=\frac{\dfrac{1}{R_{\text{ref}}A_{\text{ferro}}}\Sigma_{i=1}^{N}\left[\dfrac{\dfrac{\partial E(x,t)}{\partial P(x,t)_x}}{1+\varepsilon(x)\dfrac{\partial E(x,t)}{\partial P(x,t)_x}}\Delta x\right]}{1+\dfrac{C_{\text{ref}}}{A_{\text{ferro}}}\Sigma_{i=1}^{N}\left[\dfrac{\dfrac{\partial E(x,t)}{\partial P(x,t)_x}}{1+\varepsilon(x)\dfrac{\partial E(x,t)}{\partial P(x,t)_x}}\Delta x\right]}.$$

(The subscript x means that the differentiation is taken at constant x.)

Realistic values of $P_r(x)$, $E_c(x)$, $\varepsilon(x)$, $\sigma_0(x)$ for lead zirconate titanate (PZT)[22] (see Table I), as well as $C_{\text{ref}}=22$ nF, $R_{\text{ref}}=1$ MΩ, $A_{\text{ferro}}=250\ \mu\text{m}\times 250\ \mu\text{m}$, $L_{\text{ferro}}=800$ nm, and frequency of alternating applied voltage $f=1$ kHz from a recent article[3] were borrowed for our simulation.

TABLE I. Realistic values of $P_r(x)$, $E_c(x)$, $\varepsilon(x)$, $\sigma_0(x)$ for lead zirconate titanate, which are obtained from the graphs in Ref. 22. As the Zr composition increases from 0.25 to 0.56, both $P_r(x)$ and $E_c(x)$ decrease but $\varepsilon(x)$ increases and $\sigma_0(x)$ does not have any general trend.

Zr composition	$P_r(x)$ (μC/cm^2)	$E_c(x)$ (kV/cm)	$\varepsilon(x)/\varepsilon_0$[a]	$\sigma_0(x)$ (Ω^{-1} m^{-1})
0.25	55	75	260	2.86×10^{-11}
0.35	49	66	280	3.85×10^{-12}
0.37	47	63	300	2.22×10^{-11}
0.49	44	59	480	2.22×10^{-11}
0.56	33	43	580	1.33×10^{-11}

[a]ε_0 = dielectric permittivity of free space.

Since the mobilities of real materials can differ enormously depending on film structure, fabrication process, electric field, defects, and grain boundaries, it is difficult to obtain reliable mobility data for our simple assumption of spatially uniform mobilities.[23] As our purpose is only to demonstrate the effects of space-charge conduction on hysteresis-loop measurement, we choose to self-assign values for μ_p and μ_n, with $\mu_p < \mu_n$ and the following conditions ensured.

(a) The carrier total concentrations $[C_{\text{in}}(x)+\Delta n(x,t)]$ and $[C_{\text{in}}(x)+\Delta p(x,t)]$ are positive values throughout the simulation, where $\Delta n(x,t)$ and $\Delta p(x,t)$ are computed from the solutions of Eqs. (8) and (9), and $C_{\text{in}}(x)$ from

$$C_{\text{in}}(x)=\frac{\sigma_0(x)}{q(\mu_n+\mu_p)}. \tag{22}$$

(a) The major $E(x,t)-P(x,t)$ loop in each layer, once entered, is completely cycled every time. This is accomplished by choosing the amplitude of $V_0(t)$ to be sufficiently large.

IV. RESULTS AND DISCUSSION

By taking $\mu_p = 0.25\times10^{-8}$ cm^2 V^{-1} s^{-1} and $\mu_n = 0.25\times10^{-5}$ cm^2 V^{-1} s^{-1}, the simulation of a PZT film graded in 15 layers from 25% to 56% zirconium in the direction of increasing x (upgraded) gives an upward shifting of hysteresis loops (see Fig. 3). As the number of cycles increases, the positive and negative maxima of $E_{\text{ave}}(t)$ shift towards lower field values. This corresponds to the development of a positive average of $V_{\text{ref}}(t)$ as the hysteresis loop shifts upwards while the average of the sinusoidal $V_0(t)$ remains zero. The values of $E_{\text{ave}}(t)$ at which polarization reversal takes place remain unchanged as the cycle number increases; this is because $E_c(x)$ is a material parameter only. Several runs of the computer program indicate that the amount of hysteresis-loop shifting for higher numbers of layers is similar to the 15-layer case. The shift of $V_{\text{ref}}(t)$ in one cycle, denoted by V_{shift}, is taken as the average of the two values of $V_{\text{ref}}(t)$ that coincide with the vertical axis in the $V_{\text{ref}}(t)-E_{\text{ave}}(t)$ graph. It was found that V_{shift} develops like the typical charging-up of a capacitor and almost reaches a steady value V_{off} after about 50 cycles, with the time constant the same order of magnitude as $R_{\text{ref}}C_{\text{ref}}$ although differing by a factor of 2 (see Fig. 4). It was also found that V_{off} increases with E_{amp}, where E_{amp} is the peak-to-peak amplitude of $E_{\text{ave}}(t)$, and has

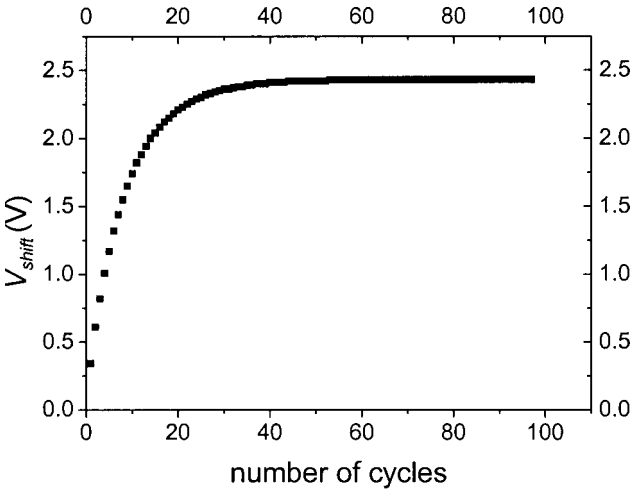

FIG. 4. Typical development of V_{shift}, which is similar to the charging-up of a capacitor.

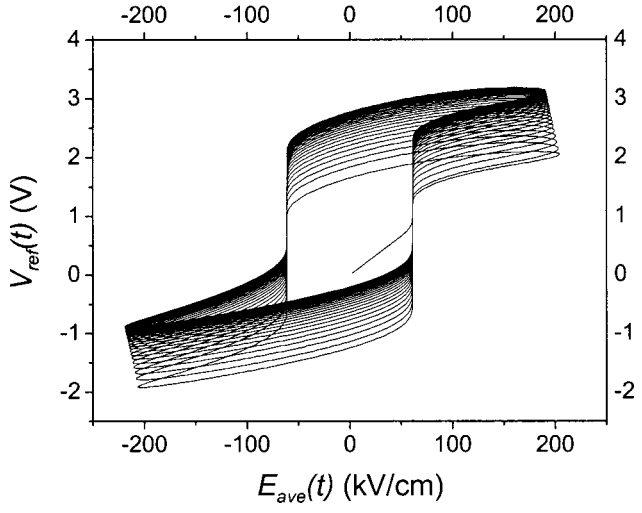

FIG. 3. The shifting of hysteresis loops when the film is upgraded.

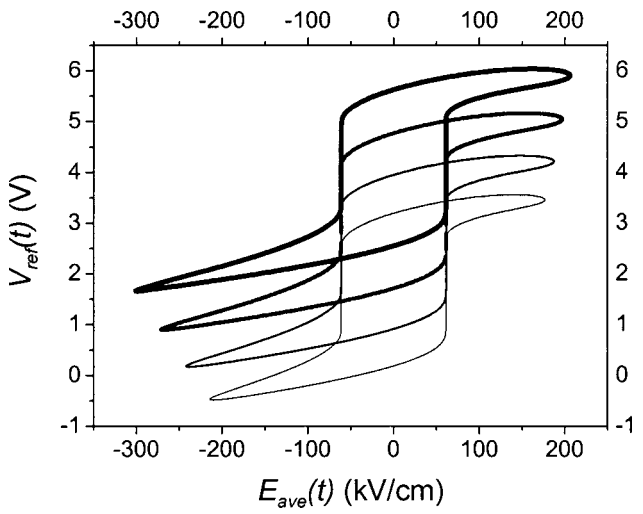

FIG. 5. The shifted hysteresis loops with their shift magnitudes V_{off} dependent on E_{amp}. Each loop is represented by a curve of different thickness.

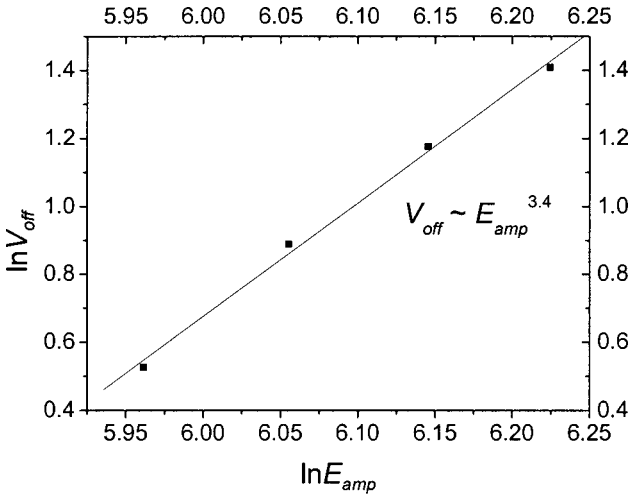

FIG. 6. V_{off} and E_{amp} approximately follow a power-law relation.

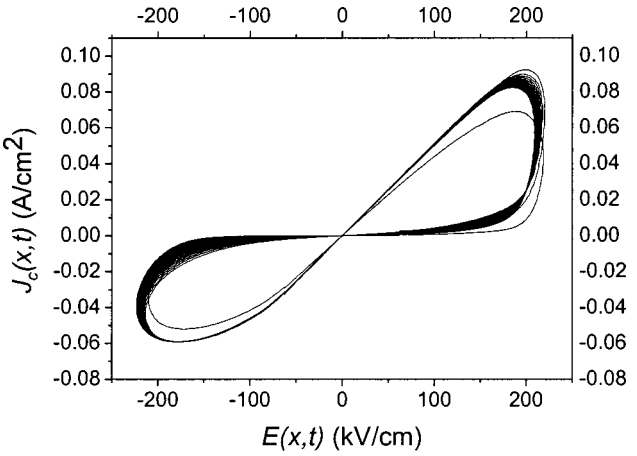

FIG. 8. Typical relation between $J_c(x,t)$ and $E(x,t)$ when the film is upgraded.

the same order of magnitude with published experimental data (a few volts)[3] (see Fig. 5). A plot of $\ln|V_{\text{off}}|$ against $\ln E_{\text{amp}}$ shows an approximate relation of $|V_{\text{off}}| \propto E_{\text{amp}}^{\gamma}$, where $\gamma \approx 3.4$ (see Fig. 6). On inverting the composition gradient (downgraded) it was found that the vertical shifting is in the downward direction, where the positive and negative maxima of $E_{\text{ave}}(t)$ shift correspondingly towards higher field values (see Fig. 7). And there is no shifting effect at all when the ferroelectric film is set to be homogeneous.

Since it has been suggested that the shifting arises from the charging-up of the reference capacitor by asymmetrical (different for positive and negative voltages) conduction currents in the ferroelectric film,[3,14] it is worth also examining whether the $J_c(x,t)-E(x,t)$ relations are asymmetrical. Interesting to note, the two quantities do not form any static relation but rather exhibit some asymmetrical hysteresis behavior for an upgraded film (see Fig. 8). It is also interesting to see that the asymmetry is reversed when the film orientation is inverted (see Fig. 9). Apart from this reverse in asymmetry, the curves in Figs. 8 and 9 are different only in the first few cycles; this is because the initial application of $E_{\text{ave}}(t)$ is, respectively, against and along the composition gradient in the upgraded and downgraded cases, leading to different space-charge profiles and, hence, different responses in the first few cycles. This initial effect fades out as the number of cycles increases; hence, the two figures eventually give the same steady-state pattern. From an integration of Eq. (19) with respect to t for one cycle, we can describe the situation as follows: In each cycle, there is a net flow of charges across the circuit, where the charges either flow across the input resistor or accumulate on the capacitor. This net flow of charges occurs because the application of $E_{\text{ave}}(t)$ is, respectively, against and along the composition gradient in positive and negative half-cycles, leading to a difference in space-charge profile and, hence, in conduction response between positive and negative half-cycles

$$\int_t^{t+T} J_0(t)\,dt = \frac{1}{A_{\text{ferro}}} \int_t^{t+T} \frac{V_{\text{ref}}(t)}{R_{\text{ref}}}\,dt + \frac{C_{\text{ref}}}{A_{\text{ferro}}}[V_{\text{ref}}(t+T) - V_{\text{ref}}(t)]. \tag{23}$$

And in each following cycle, because the capacitor voltage has a higher time average, more charges flow across the in-

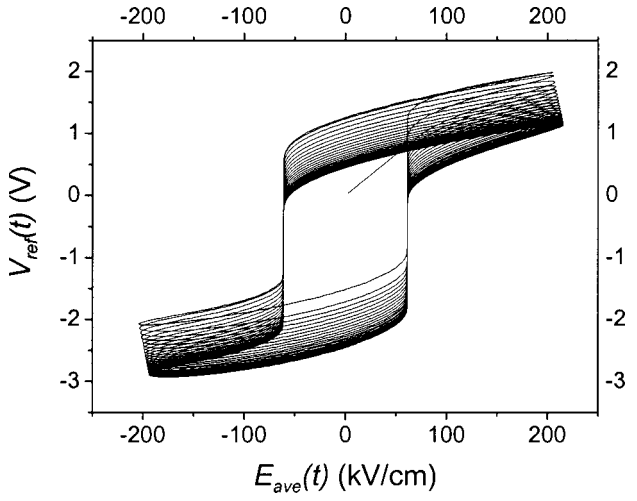

FIG. 7. The shifting of hysteresis loops when the film is downgraded.

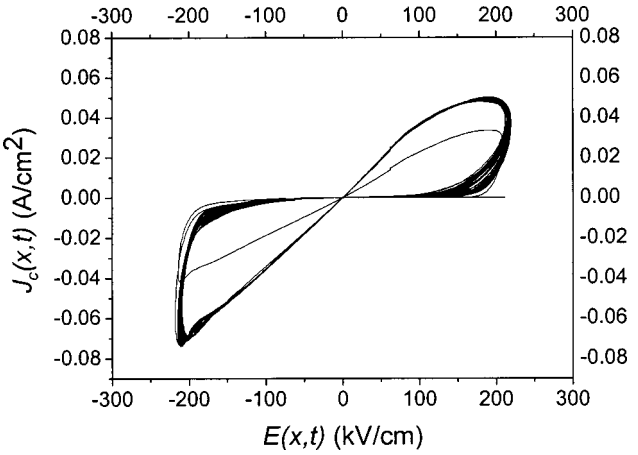

FIG. 9. Typical relation between $J_c(x,t)$ and $E(x,t)$ when the film is downgraded. Note that the asymmetry as seen in Fig. 8 is reversed.

put resistor and, hence, less accumulate on the capacitor. The process continues and finally reaches a steady condition where the net flow of charges in one cycle is all across the input resistor so that there is no further charging-up of the capacitor. This explains why V_{shift} develops in the way as shown in Fig. 4.

In our simulation, although the shapes of hysteresis loops and the power dependence of $|V_{\text{off}}|$ on E_{amp} are slightly different from those typically observed, the key features as observed in experiments are produced, namely (a) the monotonous increase of $|V_{\text{off}}|$ with E_{amp}, (b) the change in the shifting direction when the composition gradient is inverted, as well as (c) the similarity between the development of V_{shift} and the typical charging-up of a capacitor. The discrepancies between simulation and experiment can be attributed to our assumption of spatially uniform mobilities, simple Landau–Devonshire model description of hysteresis loops, as well as neglect of possible effects from electrodes and substrates. Hence, it is not unreasonable to suppose that time-dependent space-charge-limited conduction is a possible origin of the polarization offsets observed in compositionally graded ferroelectrics. Further work is needed to clarify the dependence of the offsets on gradients of remanent polarization, coercive field, dielectric constant, and temperature, as well as on temperature itself.

V. CONCLUSION

We investigated the effects of free space charges on hysteresis-loop measurement of compositionally graded ferroelectrics and found that they are quite likely to be responsible for the polarization offsets observed in experiments. Further work is needed to clarify the dependence of the offsets on gradients of different composition-related parameters and temperature, as well as on temperature itself.

ACKNOWLEDGMENTS

The work described in this article is supported by a Hong Kong Polytechnic University research grant. Special thanks are due to M. T. Lung, C. Y. Lam, and C. L. Wong for their help with our computer simulation.

APPENDIX A

The remanent polarization $P_r(x)(>0)$ can be expressed in terms of $\alpha(x)$ and $\beta(x)$ by setting $0=\alpha(x)P_r(x)+\beta(x)P_r(x)^3$, so that

$$P_r(x)^2=-\frac{\alpha(x)}{\beta(x)}. \tag{A1}$$

The polarization that corresponds to the coercive field $E_c(x)$ (>0) is denoted by $P_c(x)$ (>0) and can be determined by setting $\partial E_L(x,t)/\partial P(x,t)_x=0$ (the subscript x means that the differentiation is taken at constant x), giving

$$P_c(x)^2=-\frac{\alpha(x)}{3\beta(x)}=\frac{P_r(x)^2}{3}. \tag{A2}$$

By setting $E_c(x)=|\alpha(x)P_c(x)+\beta(x)P_c(x)^3|$ and using Eq. (A2), we get

$$E_c(x)=\frac{2\beta(x)P_r(x)^3}{3\sqrt{3}}. \tag{A3}$$

Hence,

$$\beta(x)=\frac{3\sqrt{3}E_c(x)}{2P_r(x)^3}, \tag{A4}$$

$$\alpha(x)=-\beta(x)P_r(x)^2. \tag{A5}$$

APPENDIX B

Since $D(x,t)=\varepsilon(x)E(x,t)+P(x,t)$ and $\partial E(x,t)/\partial t=[\partial E(x,t)/\partial P(x,t)_x][\partial P(x,t)/\partial t]$ (the subscript x means that the differentiation is taken at constant x), the continuity of total current can be expressed as

$$J_c(x,t)+\left[1+\varepsilon(x)\frac{\partial E(x,t)}{\partial P(x,t)_x}\right]\frac{\partial P(x,t)}{\partial t}=\frac{V_{\text{ref}}(t)}{R_{\text{ref}}A_{\text{ferro}}}+\frac{C_{\text{ref}}}{A_{\text{ferro}}}\frac{dV_{\text{ref}}(t)}{dt}. \tag{B1}$$

Using the chain rule again and Eq. (B1), we get

$$\frac{\partial E(x,t)}{\partial t}=\frac{\partial E(x,t)}{\partial P(x,t)_x}\frac{\frac{V_{\text{ref}}(t)}{R_{\text{ref}}A_{\text{ferro}}}+\frac{C_{\text{ref}}}{A_{\text{ferro}}}\frac{dV_{\text{ref}}(t)}{dt}-J_c(x,t)}{1+\varepsilon(x)\frac{\partial E(x,t)}{\partial P(x,t)_x}}. \tag{B2}$$

The vanishing of voltage sum around a closed loop gives

$$\int_0^{L_{\text{ferro}}}\frac{\partial E(x,t)}{\partial t}dx=\frac{dV_0(t)}{dt}-\frac{dV_{\text{ref}}(t)}{dt}. \tag{B3}$$

Combining Eqs. (B2) and (B3), we write

$$\begin{aligned}\frac{dV_0(t)}{dt}-\frac{dV_{\text{ref}}(t)}{dt}&=\frac{V_{\text{ref}}(t)}{R_{\text{ref}}A_{\text{ferro}}}\int_0^{L_{\text{ferro}}}\frac{\frac{\partial E(x,t)}{\partial P(x,t)_x}}{1+\varepsilon(x)\frac{\partial E(x,t)}{\partial P(x,t)_x}}dx\\&+\frac{C_{\text{ref}}}{A_{\text{ferro}}}\frac{dV_{\text{ref}}(t)}{dt}\int_0^{L_{\text{ferro}}}\frac{\frac{\partial E(x,t)}{\partial P(x,t)_x}}{1+\varepsilon(x)\frac{\partial E(x,t)}{\partial P(x,t)_x}}dx\\&-\int_0^{L_{\text{ferro}}}\frac{J_c(x,t)\frac{\partial E(x,t)}{\partial P(x,t)_x}}{1+\varepsilon(x)\frac{\partial E(x,t)}{\partial P(x,t)_x}}dx\end{aligned} \tag{B4}$$

and get

$$\begin{aligned}dV_{\text{ref}}(t)&=V_{\text{ref}}(t+dt)-V_{\text{ref}}(t)\\&=[f_1(t)-V_{\text{ref}}(t)f_2(t)]dt,\end{aligned} \tag{B5}$$

where

$$f_1(t)=\frac{\dfrac{dV_0(t)}{dt}+\int_0^{L_{\text{ferro}}}\dfrac{J_c(x,t)\dfrac{\partial E(x,t)}{\partial P(x,t)_x}}{1+\varepsilon(x)\dfrac{\partial E(x,t)}{\partial P(x,t)_x}}dx}{1+\dfrac{C_{\text{ref}}}{A_{\text{ferro}}}\int_0^{L_{\text{ferro}}}\dfrac{\dfrac{\partial E(x,t)}{\partial P(x,t)_x}}{1+\varepsilon(x)\dfrac{\partial E(x,t)}{\partial P(x,t)_x}}dx} \quad \text{and}$$

$$f_2(t)=\frac{\dfrac{1}{R_{\text{ref}}A_{\text{ferro}}}\int_0^{L_{\text{ferro}}}\dfrac{\dfrac{\partial E(x,t)}{\partial P(x,t)_x}}{1+\varepsilon(x)\dfrac{\partial E(x,t)}{\partial P(x,t)_x}}dx}{1+\dfrac{C_{\text{ref}}}{A_{\text{ferro}}}\int_0^{L_{\text{ferro}}}\dfrac{\dfrac{\partial E(x,t)}{\partial P(x,t)_x}}{1+\varepsilon(x)\dfrac{\partial E(x,t)}{\partial P(x,t)_x}}dx}.$$

After replacing dx and dt by Δx and Δt, respectively, we get Eq. (21).

[1] N. W. Schubring, J. V. Mantese, A. L. Micheli, A. B. Catalan, and R. J. Lopez, Phys. Rev. Lett. **68**, 1778 (1992).
[2] C. B. Sawyer and C. H. Tower, Phys. Rev. **35**, 269 (1930).
[3] R. Bouregba, G. Poullain, B. Vilquin, and G. Le Rhun, J. Appl. Phys. **93**, 5583 (2003).
[4] J. V. Mantese, N. W. Schubring, A. L. Micheli, A. B. Catalan, M. S. Mohammed, R. Naik, and G. W. Auner, Appl. Phys. Lett. **71**, 2047 (1997).
[5] M. Brazier, M. McElfresh, and S. Mansour, Appl. Phys. Lett. **72**, 1121 (1998).
[6] Z. Chen, K. Arita, M. Lim, and C. A. Paz De Araujo, Integr. Ferroelectr. **24**, 181 (1999).
[7] D. Bao, N. Wakiya, K. Shinozaki, N. Mizutani, and X. Yao, J. Appl. Phys. **90**, 506 (2001).
[8] T. Matsuzaki and H. Funakubo, J. Appl. Phys. **86**, 4559 (1999).
[9] D. Bao, X. Yao, and L. Zhang, Appl. Phys. Lett. **76**, 2779 (2000).
[10] D. Bao, N. Mizutani, L. Zhang, and X. Yao, J. Appl. Phys. **89**, 801 (2001).
[11] D. Bao, N. Mizutani, X. Yao, and L. Zhang, Appl. Phys. Lett. **77**, 1041 (2000).
[12] D. Bao, N. Mizutani, X. Yao, and L. Zhang, Appl. Phys. Lett. **77**, 1203 (2000).
[13] M. Brazier, M. McElfresh, and S. Mansour, Appl. Phys. Lett. **74**, 299 (1999).
[14] G. Poullain, R. Bouregba, B. Vilquin, G. Le Rhun, and H. Murray, Appl. Phys. Lett. **81**, 5015 (2002).
[15] W. Fellberg, J. V. Mantese, N. W. Schubring, and A. L. Micheli, Appl. Phys. Lett. **78**, 524 (2001).
[16] S. P. Alpay, Z. G. Ban, and J. V. Mantese, Appl. Phys. Lett. **82**, 1269 (2003).
[17] R. Coelho, *Physics of Dielectrics for the Engineer* (Elsevier Scientific, New York, 1979), pp. 123–125.
[18] C. K. Wong, Y. W. Wong, and F. G. Shin, J. Appl. Phys. **92**, 3974 (2002).
[19] Y. T. Or, C. K. Wong, B. Ploss, and F. G. Shin, J. Appl. Phys. **93**, 4112 (2003).
[20] Y. T. Or, C. K. Wong, B. Ploss, and F. G. Shin, J. Appl. Phys. **94**, 3319 (2003).
[21] M. E. Lines and A. M. Glass, *Principles and Applications of Ferroelectrics and Related Materials* (Clarendon, Oxford, 1977).
[22] C. M. Foster, G. R. Bai, R. Csencsits, J. Vetrone, R. Jammy, L. A. Wills, E. Carr, and J. Amano, J. Appl. Phys. **81**, 2349 (1997).
[23] Dr. D. P. Chu from Department of Engineering, University of Cambridge, UK (private communication).